

A Comparison of Sound Field Synthesis Techniques for Non-Smooth Secondary Source Distributions*

Fiete Winter and Sascha Spors

Institute of Communications Engineering, University of Rostock, R.-Wagner-Str. 31 (H8), D-18119 Rostock, Germany

Email: {fiete.winter, sascha.spors}@uni-rostock.de

Introduction

Sound Field Synthesis (SFS) techniques reproduce a virtual sound field inside an extended listening area using a distribution of loudspeakers located on the area's boundary. The theoretical foundations of such techniques assume a spatially smooth boundary. Non-smooth shapes, like e.g. rectangles, are however more suitable in practical applications since the loudspeaker setup has to fit into the architecture of the listening room. Such discrepancy introduces diffraction artefacts to the reproduced sound field. Consequentially, deviations from the desired sound field with respect to amplitude and spectral properties are present.

This paper compares Wave Field Synthesis [1], Local Wave Field Synthesis [2], and an analytically derived solution for rectangular geometries [3] regarding the mentioned artefacts. First, the reproduction scenario is presented. The used techniques for SFS are then described and compared followed by a conclusion.

Reproduction Scenario

The reproduction scenario used in this comparison is a rectangular listening area Ω located in the horizontal plane (i.e. $z = 0$). This area is surrounded by four linear segments of 16 equidistantly placed loudspeakers, each (Fig. 1). The loudspeakers are indexed in a counter-clockwise manner starting at the bottom right (cf. numbers). The distance between the first and the last loudspeaker of each segment amounts to $L = 4$ metres. All adjacent loudspeakers including the ones at the corners have the same euclidean distance to each other. The sound field emitted by an individual loudspeaker located at $\mathbf{x}_0 = \rho_0[\cos(\phi_0), \sin(\phi_0), 0]^T$ is modelled by the three-dimensional free-field Green's function

$$G(\mathbf{x}|\mathbf{x}_0, \omega) = G(\mathbf{x}|\mathbf{x}_0) = \frac{e^{-jk|\mathbf{x}-\mathbf{x}_0|}}{4\pi|\mathbf{x}-\mathbf{x}_0|} \quad (1)$$

The virtual sound field $S(\mathbf{x})$ which is to be reproduced is a point source located at $\mathbf{x}_s = \rho_s[\cos \phi_s, \sin \phi_s, 0]^T$ with a constant radius $\rho_s = 4$ metres. Its sound field is analogously described by $G(\mathbf{x}|\mathbf{x}_s)$.

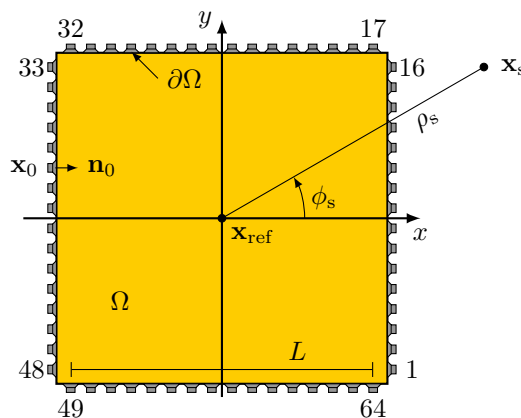


Figure 1: Reproduction Scenario

Sound Field Synthesis Techniques

The problem of SFS can be mathematically formulated in terms of the Single Layer Potential (SLP) [11, Ch. 2]

$$P(\mathbf{x}) = \oint_{\partial\Omega} D(\mathbf{x}_0)G(\mathbf{x}|\mathbf{x}_0) dA(\mathbf{x}_0) \stackrel{!}{=} S(\mathbf{x}), \quad (2)$$

where $dA(\mathbf{x}_0)$ denotes a suitably chosen boundary element for the integration over $\partial\Omega$. Eq. (2) defines the reproduced sound field $P(\mathbf{x})$ as the superposition of the sound fields $G(\mathbf{x}|\mathbf{x}_0)$ emitted by the respective secondary source located at $\mathbf{x}_0 \in \partial\Omega$. In order to achieve agreement between $P(\mathbf{x})$ and $S(\mathbf{x})$ each secondary source is individually driven by its driving function $D(\mathbf{x}_0)$. As the secondary source distribution is restricted to the horizontal plane (2.5D synthesis), the resulting dimensionality mismatch causes an undesired amplitude decay in the reproduced sound field. Correct synthesis can only be achieved at a reference point \mathbf{x}_{ref} . In the next sub-sections three techniques defining a suitable driving function $D(\mathbf{x}_0)$ to reproduce the desired sound field are introduced.

Equivalent Scattering Approach (ESA)

It is known [4, Sec. 8.7], that the driving function for (2) can be derived by solving an equivalent scattering problem: The virtual sound field $S(\mathbf{x})$ is scattered by a sound-soft (pressure-release) obstacle, whose surface coincides with $\partial\Omega$. The directional gradient of the resulting, total sound pressure on the scatterer's surface is then equivalent to the desired driving function $D_0(\mathbf{x}_0)$. Although a solution for a rectangular scatterer is not known to the authors, a solution for a sound-hard semi-infinite edge (cf. Fig. 2a) located at the coordinates origin was derived in [5, Sec. 10.1] and was further extended to the

*This research has been supported by EU FET grant Two!EARS, ICT-618075.

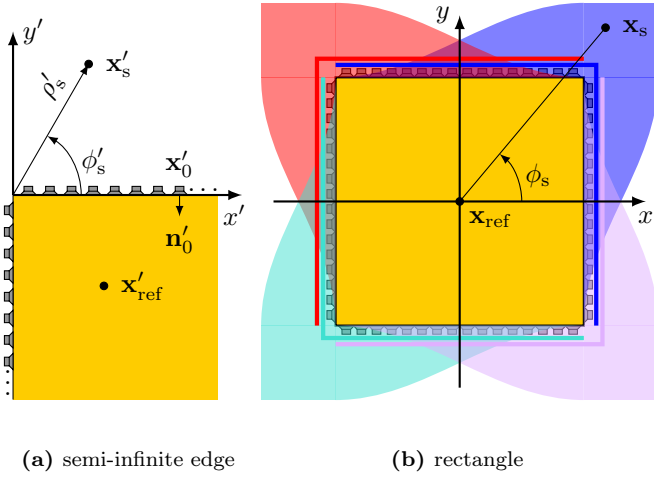


Figure 2: (a) shows the underlying geometry for (3). (b) illustrates the strategy to cross-fade the driving functions of each corner (encoded in the different colors). For the transition between two corners, a cosine cross-fading depending on the x - or y -coordinate of the virtual sound source is applied to the two involved driving functions.

sound-soft case in [3]. The corresponding driving function is given as [3]

$$D_{\text{ESA}}(\mathbf{x}'_0, \omega) = -j \frac{2}{3} a_{\text{ESA}}(\mathbf{x}'_0) \sqrt{\frac{|\mathbf{x}'_{\text{ref}} - \mathbf{x}'_0|}{|\mathbf{x}'_{\text{ref}} - \mathbf{x}'_s|}} \quad (3)$$

$$\sum_{n=0}^{\infty} \frac{1}{\epsilon_n} \cos(\nu \phi'_0) \sin(\nu \phi'_s) \frac{\nu}{\rho_0} J_{\nu}(k \rho'_{<}) H_{\nu}^{(2)}(k \rho'_{>})$$

with $\nu = \frac{2}{3}n$ and $\epsilon_n = 1 + \delta_{n0}$, where δ_{n0} is the Kronecker delta. The auxiliary radii are defined as $\rho'_{<} = \min(\rho'_0, \rho'_s)$ and $\rho'_{>} = \max(\rho'_0, \rho'_s)$. Furthermore, the secondary source selection criterion

$$a_{\text{ESA}}(\mathbf{x}'_0) = \begin{cases} 1 & , \text{ if } \phi'_0 = 0. \\ -1 & , \text{ if } \phi'_0 = \frac{3}{2}\pi. \\ 0 & , \text{ otherwise,} \end{cases} \quad (4)$$

for the Equivalent Scattering Approach (ESA) ensures that only secondary source belonging to the semi-infinite edge are active. Note, that (3) is only valid for source azimuths $\phi_s \in [0, 3\pi/2]$. For a distinct range of virtual source positions, the scattering properties of a rectangle's corner including its adjacent linear segments can be reasonably approximated by that of a shifted and rotated semi-infinite edge. Here, the approximation lies in the truncation of the linear segments due to the other corners. Each corner is treated separately and the resulting driving functions are combined via a sensible selection and cross-fading (cf. Fig. 2b). For the a distinct corner, the coordinate system has to be shifted and rotated in order to make (3) applicable.

Wave Field Synthesis (WFS)

Wave Field Synthesis (WFS) is a well-established method for SFS. The underlying theory was developed by Berkhout et al. [1] at the Delft University of Technology.

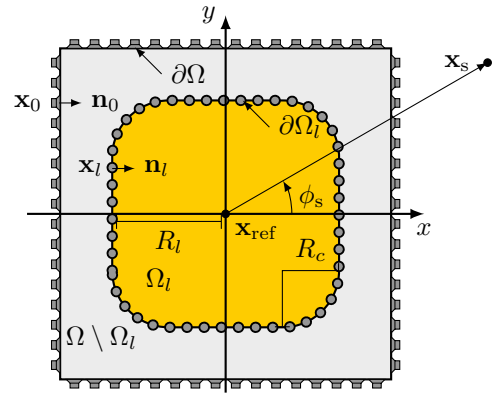


Figure 3: Parametrisation of Local Wave Field Synthesis

The driving function for a virtual point source located at \mathbf{x}_s is given as [6, Eq. (3.10-11)]

$$D_{\text{WFS}}(\mathbf{x}_0) = \sqrt{\frac{jk}{2\pi}} \sqrt{\frac{|\mathbf{x}_{\text{ref}} - \mathbf{x}_0|}{|\mathbf{x}_{\text{ref}} - \mathbf{x}_0| + |\mathbf{x}_s - \mathbf{x}_0|}} \quad (5)$$

$$a_{\text{WFS}}(\mathbf{x}_0) \frac{\mathbf{n}_0^T(\mathbf{x}_s - \mathbf{x}_0)}{|\mathbf{x}_s - \mathbf{x}_0|^{3/2}} e^{-jk|\mathbf{x}_s - \mathbf{x}_0|}.$$

The secondary source selection criterion [7, Eq. (15)]

$$a_{\text{WFS}}(\mathbf{x}_0) = \begin{cases} 1 & , \text{ if } \mathbf{n}_0^T(\mathbf{x}_0 - \mathbf{x}_s) \geq 0, \\ 0 & , \text{ otherwise,} \end{cases} \quad (6)$$

ensures that only those secondary sources are active where the propagation direction of the virtual point source at the position \mathbf{x}_0 has a positive component direction of the normal vector \mathbf{n}_0 [7, Sec. 2.4].

Local Wave Field Synthesis (LWFS)

The original goal of Local Wave Field Synthesis (LWFS) [2] was to decrease spatial aliasing artefacts and thus increase the accuracy of the synthesised sound field within a small, local listening area while allowing stronger artefacts outside. For a detailed analysis of the physical properties of this approach the reader is referred to [8, 9]. LWFS can also be utilized to reduce the effects of the non-smooth boundary $\partial\Omega$ by defining a smoother boundary $\partial\Omega_l$ for the local listening area Ω_l (cf. Fig. 3). Within this publication a rounded rectangle with radius R_l and corner radius R_c is used in order to study the influence of the boundaries' smoothness. Note, that $R_c = 0$ and $R_c = R_l$ result in a rectangular and a circular boundary, respectively.

In order to reproduce the virtual sound field inside Ω_l , a set of focused sources is utilised as a so-called *virtual secondary source distribution* along $\partial\Omega_l$ (cf. grey dots in Fig. 3). These sources are driven like a real loudspeaker setup, e.g. by WFS. The driving function $D_{\text{WFS}}(\mathbf{x}_l)$ for a virtual secondary source located at $\mathbf{x}_l \in \partial\Omega_l$ is derived by substituting \mathbf{x}_0 and \mathbf{n}_0 in (5) with \mathbf{x}_l and \mathbf{n}_l . Each focused source is reproduced by the real loudspeaker distribution. The corresponding WFS driving function is

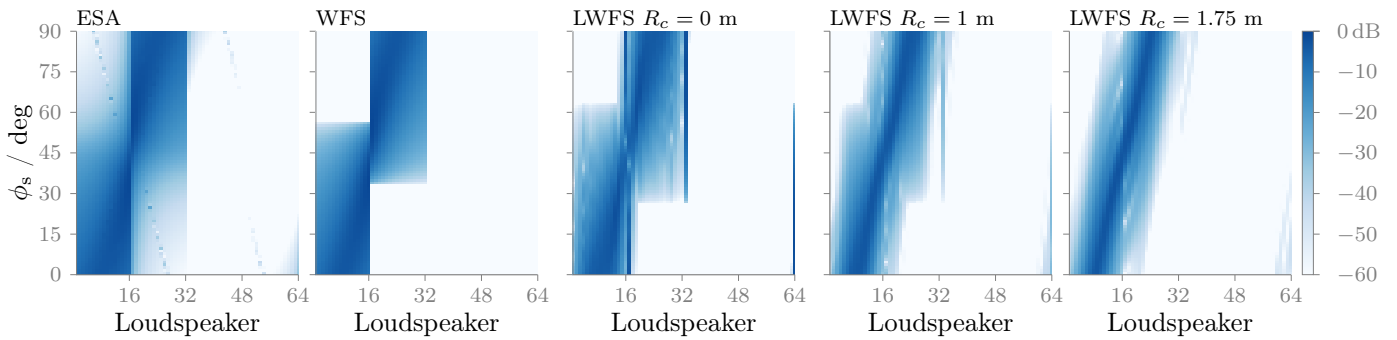


Figure 4: Magnitude of the driving functions to synthesize a monochromatic ($f = 500$ Hz) virtual point source for all loudspeakers and various source azimuths ϕ_s .

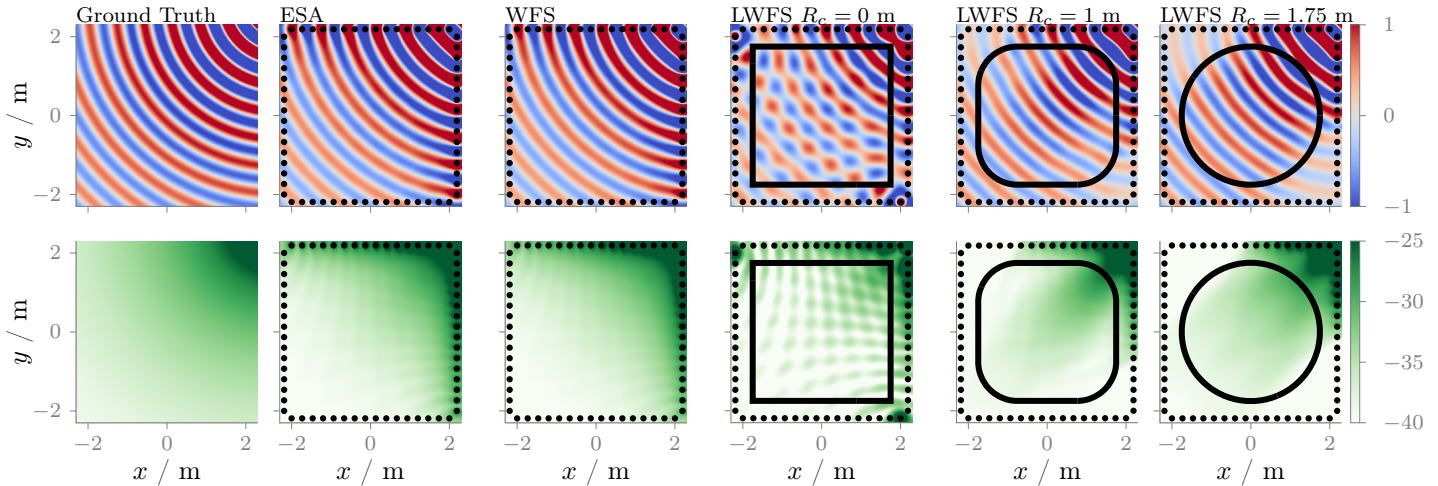


Figure 5: The plots in the first column show the real part and the magnitude of a monochromatic ($f = 500$ Hz) point source located at $\phi_s = 45$ degrees and $\rho_s = 4$ metre. The remaining plots show the same quantities of the reproduced sound field using the rectangular secondary source distribution driven by different SFS techniques.

given as [10, Eq. (A-14)]

$$D_{fs}(\mathbf{x}_0, \mathbf{x}_l) = \sqrt{\frac{-jk}{2\pi}} \sqrt{\left| \frac{|\mathbf{x}_{ref} - \mathbf{x}_0|}{|\mathbf{x}_{ref} - \mathbf{x}_0| - |\mathbf{x}_l - \mathbf{x}_0|} \right|} \quad (7)$$

$$a_{fs}(\mathbf{x}_0, \mathbf{x}_l) \frac{\mathbf{n}_0^T(\mathbf{x}_l - \mathbf{x}_0)}{|\mathbf{x}_l - \mathbf{x}_0|^{3/2}} e^{+jk|\mathbf{x}_l - \mathbf{x}_0|}.$$

The secondary source selection criterion

$$a_{fs}(\mathbf{x}_0, \mathbf{x}_l) = \begin{cases} \frac{\mathbf{n}_l^T(\mathbf{x}_l - \mathbf{x}_0)}{|\mathbf{x}_l - \mathbf{x}_0|} & , \text{ if } \mathbf{n}_l^T(\mathbf{x}_l - \mathbf{x}_0) \geq 0, \\ 0 & , \text{ otherwise,} \end{cases} \quad (8)$$

is a modified version of [8, Eq. (4)]. Here, the originally used rectangular window is replaced by a cosine shaped one. Finally, the resulting driving function

$$D_{LWFS}(\mathbf{x}_0) = \oint_{\partial\Omega_l} D_{WFS}(\mathbf{x}_l) D_{fs}(\mathbf{x}_0, \mathbf{x}_l) dA_l(\mathbf{x}_l) \quad (9)$$

constitutes a superposition of the driving functions to reproduce a single focused source weighted by the driving function for the focused source to reproduced the virtual sound field inside Ω_l . Note, that the integral migrates to a summations over a finite set of positions \mathbf{x}_l for practical implementations. Within this study, a set of 256 virtual secondary sources is positioned equidistantly along $\partial\Omega_l$.

Comparison

The magnitude of the different driving functions is shown in Fig. 4. For WFS, an abrupt activation/deactivation of the first (1-16) and second (17-32) linear loudspeaker segments can be observed as the virtual point source is rotated around the adjacent corner. This is due to the secondary source selection criterion (6): Contrary to the ESA, WFS only selects secondary sources which are directly *illuminated* [11, p. 29/30] by the virtual point source. It neglects diffraction effects around the corners, which are most prominent at low frequencies. Thus WFS constitutes a high-frequency approximation of the SLP. The last three plots in Fig. 4 illustrate the influence of the smoothness of the local listening area on the LWFS driving functions: As the corner radius R_c of the local listening area $\partial\Omega_l$ increases, the discontinuities vanish more and more. For a rectangular area, the driving functions' structure closely resemble for LWFS and WFS. For a circular area, the LWFS driving function is smeared over many loudspeakers. For two distinct virtual source azimuths ϕ_s , the driving functions are approximately shifted copies of the each other as the circular geometry is invariant w.r.t. the rotation of the virtual point source.

It is shown in Fig. 5, that all methods achieve a phase correct synthesis of the virtual sound field. However, LWFS with $R_c = 0$ introduces considerable magnitude

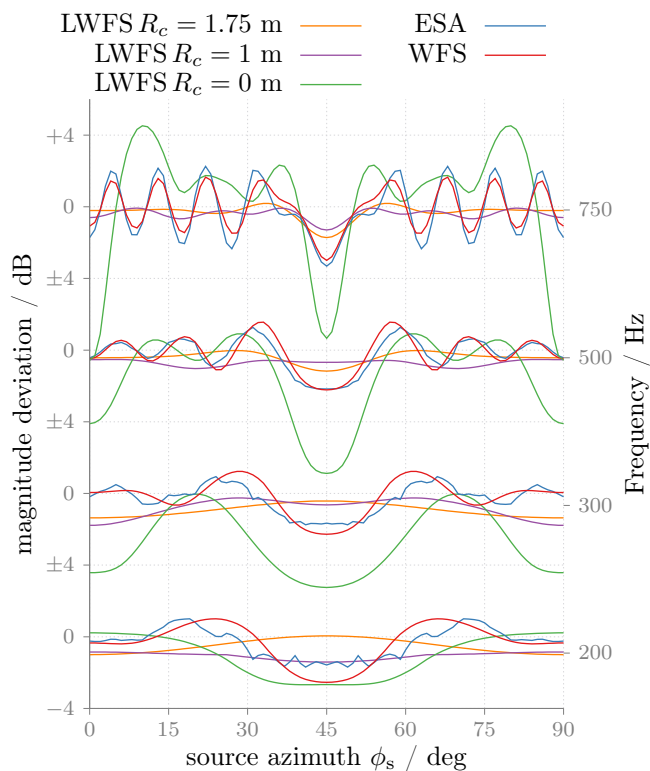


Figure 6: Magnitude deviations from $S(\mathbf{x}_{\text{ref}})$ are plotted against the virtual source azimuth ϕ_s for different SFS methods and temporal frequencies.

fluctuations. This observation is further confirmed by the strongly varying magnitude at the reference point \mathbf{x}_{ref} shown in Fig. 6. The results furthermore suggests, that a smooth local listening area reduces this variation noticeable. Although the ESA states the close-to-exact solution of the SLP for the rectangular geometry, no significant improvement compared to WFS can be observed in Fig. 6. As already discussed in [3], ESA requires densely placed secondary sources near the corners in order to achieve correct synthesis. As the driving function (3) exhibits a inverse proportional dependency w.r.t the distance ρ'_0 , the presented reproduction setup with missing corner loudspeaker lacks considerable amount of magnitude for this approach.

Finally, the trade-off between available listening area and magnitude deviation is analysed for various LWFS parametrization: As observable in Fig. 7, the radius R_l has only minor influence on the magnitude errors, as these are primarily determined by the smoothness of $\partial\Omega_l$ and thus by R_c . This suggests, that a decreased listening area due to a high R_c is more effective than due to a small R_l w.r.t. the reproduction of magnitude errors.

Conclusion

This work presented a comparison of three Sound Field Synthesis approaches for a particular reproduction scenario using a rectangular array of 64 loudspeakers. Local Wave Field Synthesis is able to reduce the amplitude fluctuations arising from the discontinuities at the rectangles corners. This can however only be done at the cost a smaller listening area.

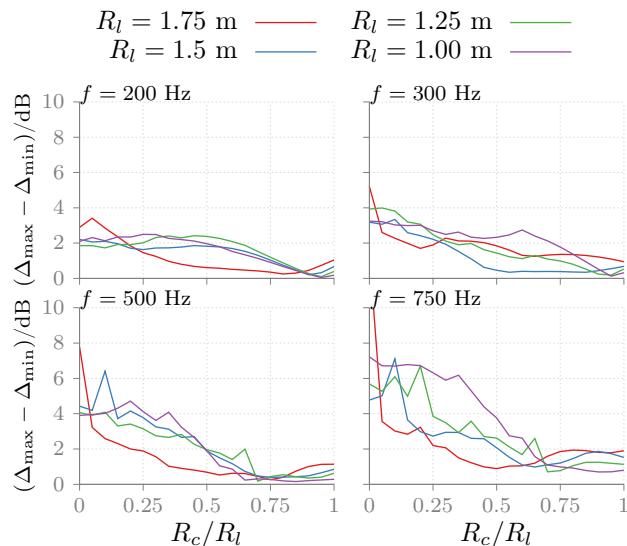


Figure 7: The difference between the minimum (Δ_{\min}) and the maximum (Δ_{\max}) deviation at the reference point over all ϕ_s for different LWFS parametrizations is plotted against the respective ratio of R_c and R_l . R_c is varied from 0 to R_l .

References

- [1] A. J. Berkhout. “A Holographic Approach to Acoustic Control”. In: *J. Aud. Eng. Soc.* 36.12 (1988), pp. 977–995.
- [2] S. Spors and J. Ahrens. “Local Sound Field Synthesis by Virtual Secondary Sources”. In: *Proc. of 40th Intl. Aud. Eng. Soc. Conf. on Spatial Audio*. Tokyo, Japan, 2010.
- [3] S. Spors and F. Schultz. “Improved Driving Functions for Rectangular Loudspeaker Arrays Driven by Sound Field Synthesis”. In: *German Annual Conference on Acoustics (DAGA)*. Aachen, Germany, 2016.
- [4] E. G. Williams. *Fourier Acoustics: Sound Radiation and Nearfield Acoustical Holography*. London: Academic Press, 1999.
- [5] M. Möser. *Technische Akustik*. 10th ed. Springer, 2015.
- [6] E. W. Start. “Direct Sound Enhancement by Wave Field Synthesis”. PhD thesis. Delft University of Technology, 1997.
- [7] S. Spors, R. Rabenstein, and J. Ahrens. “The theory of Wave Field Synthesis revisited”. In: *Proc. of 124th Aud. Eng. Soc. Conv.* Amsterdam, The Netherlands, 2008.
- [8] F. Winter and S. Spors. “Physical Properties of Local Wave Field Synthesis using Linear Loudspeaker Arrays”. In: *Proc. of 138th Aud. Eng. Soc. Conv.* Warsaw, Poland, 2015.
- [9] F. Winter and S. Spors. “Physical Properties of Local Wave Field Synthesis using Circular Loudspeaker Arrays”. In: *EuroNoise*. Vol. 31. c. Maastricht, The Netherlands, 2015, pp. 263–268.
- [10] E. N. G. Verheijen. “Sound Reproduction by Wave Field Synthesis”. PhD thesis. Delft University of Technology, 1997.
- [11] J. Ahrens. “The Single-layer Potential Approach Applied to Sound Field Synthesis Including Cases of Non-enclosing Distributions of Secondary Sources”. PhD thesis. Berlin, Germany: Technische Universität Berlin, 2010.